

the use of the HP4192A. They would also like to thank HemoBanco for helping them in preparing the blood samples. Finally, they would like to thank Lic. C. Protto for preparing the solutions and to Dr. A. Coviello, Dr. S. Jerez, and Dr. G. Orce for their useful discussions and contributions.

## REFERENCES

- [1] J. Z. Ma, J. Ebben, H. Xia, and A. J. Collins, "Hematocrit level and associated mortality in hemodialysis patients," *J. Amer. Soc. Nephrol.*, vol. 10, pp. 610–619, 1999.
- [2] A. Aris, J. M. Padro, J. O. Bonnin, and J. M. Caralps, "Prediction of hematocrit changes in open-heart surgery without blood transfusion," *J. Cardiovasc. Surg.*, vol. 25, no. 6, pp. 545–548, Nov-Dec. 1984.
- [3] J. P. Morucci, M. E. Valentinuzzi, B. Rigaud, C. J. Felice, N. Chaveau, and P. M. Marsili, "Bioelectrical impedance technique in medicine," *CRC Crit. Rev. Biomed. Eng.*, vol. 24, no. 4–6, pp. 209–681, 1996.
- [4] J. E. Yardley, D. B. Kell, J. Barrett, and C. L. Davey, "On-line, real-time measurements of cellular biomass using dielectric spectroscopy," *Biotechnol. Genet. Eng. Rev.*, vol. 17, pp. 3–35, 2000.
- [5] M. Maasrani, M. Y. Jaffrin, and B. Boudailliez, "Continuous measurements by impedance of haematocrit and plasma volume variations during dialysis," *Med. Biol. Eng. Comput.*, vol. 35, no. 3, pp. 167–171, May 1997.
- [6] P. M. de Vries, J. W. Langendijk, P. M. Kouw, V. Visser, and H. Schneider, "Implications of the dielectrical behavior of human blood for continuous online measurement of haematocrit," *Med. Biol. Eng. Comput.*, vol. 31, no. 5, pp. 445–448, Sep. 1993.
- [7] C. G. Olthof, P. M. Kouw, A. J. Donker, J. J. De Lange, and P. M. de Vries, "Non-invasive conductivity technique to detect changes in haematocrit: *In vitro* validation," *Med. Biol. Eng. Comput.*, vol. 32, no. 5, pp. 495–500, Sep. 1994.
- [8] T. X. Zhao, B. Jacobson, and T. Ribbe, "Triple-frequency method for measuring blood impedance," *Physiol. Meas.*, vol. 14, no. 2, pp. 145–156, May 1993.
- [9] K. Cha, R. G. Farris, E. F. Brown, and D. W. Wilmore, "An electronic method for rapid measurement of haematocrit in blood samples," *Physiol. Meas.*, vol. 15, no. 2, pp. 129–137, May 1994.
- [10] M. Y. Jaffrin and C. Fournier, "Comparison of optical, electrical, and centrifugation techniques for haematocrit monitoring of dialyzed patients," *Med. Biol. Eng. Comput.*, vol. 37, no. 4, pp. 433–439, July 1994.
- [11] K. R. Foster and H. P. Schwan, "Dielectric properties of tissues and biological materials: A critical review," *CRC Crit. Rev. Biomed. Eng.*, vol. 17, no. 1, pp. 25–104, 1989.
- [12] T. X. Zhao, "Electrical impedance and haematocrit of human blood with various anticoagulants," *Physiol. Meas.*, vol. 14, no. 3, pp. 299–307, Aug. 1993.
- [13] E. F. Treo, D. O. Cervantes, C. J. Felice, M. C. Tirado, and M. E. Valentinuzzi, "Hematocrit measurement by dielectric spectroscopy," in *Proc. 2nd Joint Meeting IEEE-EMBS/BMES*, vol. 2, Houston, TX, 2002, pp. 1750–1751.
- [14] C. Grosse and M. C. Tirado, "Measurement of the dielectric properties of polystyrene particles in electrolyte solution," in *Proc. Mat. Res. Soc. Symp.*, vol. 340, 1996, pp. 287–293.
- [15] L. A. Geddes and L. E. Baker, *Principles of Applied Biomedical Instrumentation*. New York: Wiley, 1989.
- [16] H. Beving, L. E. Eriksson, C. L. Davey, and D. B. Kell, "Dielectric properties of human blood and erythrocytes at radio frequencies (0.2–10 MHz); dependence on cell volume fraction and medium composition," *Eur. Biophys. J.*, vol. 23, no. 3, pp. 207–215, 1994.
- [17] M. Y. Jaffrin, M. Maasrani, A. Le Gourrier, and B. Boudailliez, "Extra- and intracellular volume monitoring by impedance during haemodialysis using Cole-Cole extrapolation," *Med. Biol. Eng. Comput.*, vol. 35, no. 3, pp. 266–270, May 1997.
- [18] H. Fricke, "Relation of the permittivity of biological cell suspensions to fractional cell volume," *Nature*, vol. 172, pp. 731–732, 1953.

## Navigator Echo Motion Artifact Suppression in Synthetic Aperture Ultrasound Imaging

Yasser M. Kadah, Abd El-Monem El-Sharkawy, and  
Abou-Bakr M. Youssef

**Abstract**—We develop a simple yet effective technique for motion artifact suppression in ultrasound images reconstructed from multiple acquisitions. Assuming a rigid-body motion model, a navigator echo is computed for each acquisition and then registered to estimate the motion in between acquisitions. By detecting this motion, it is possible to compensate for it in the reconstruction step to obtain images that are free of lateral motion artifacts. The theory and practical implementation details are described and the performance is analyzed using computer simulations as well as real data. The results indicate the potential of the new method for real-time implementation in lower cost ultrasound imaging systems.

**Index Terms**—Information theoretic image enhancement, motion artifact, navigator echo, synthetic aperture.

### I. INTRODUCTION

The lateral resolution of ultrasound imaging scales directly with the aperture size. Therefore, the aperture is improved by increasing the number of array elements used to collect the ultrasound echoes for a given element size. Phased array systems represent an optimal solution where all array elements are used in signal transmission and reception to achieve the best possible lateral resolution. This class of ultrasound imaging systems represents the high-end of the market given the complexity of the beamforming involved. In less expensive ultrasound imaging systems, however, only a small number of independent channels is utilized to collect ultrasound echoes in order to reduce the system complexity and consequently its cost. This results in degradation of image lateral resolution and hence limits the diagnostic value of the output images. As a result, synthetic aperture imaging was developed to enhance the spatial resolution employing the same number of channels [1]. The basic idea of this technique is to acquire the desired aperture through multiple acquisitions where such acquisitions are combined to form an effective aperture size that is larger than the original. This can be further generalized to include interleaved acquisition (i.e., reconstruction from consecutive even and odd field acquisitions) and averaging where image reconstruction is performed from multiple acquisitions.

Since multiple acquisitions of the same structures must be done at different times, it is likely that the field of view may move in between consecutive acquisitions due to either tissue motion or probe motion. Hence, ultrasound images reconstructed from such acquisitions may contain motion artifacts. Such motion artifacts can be rather severe and limit the diagnostic value of the reconstructed images in some cases.

Manuscript received April 27, 2003; revised May 9, 2004. This work was supported in part by the R&D department at International Electronics—Biomedical Division (currently IBE Tech), Giza, Egypt. Asterisk indicates corresponding author.

\*Y. M. Kadah, is with the Biomedical Engineering Department, Cairo University, Giza 12613, Egypt and the Georgia Tech/Emory Department of Biomedical Engineering, Atlanta, GA 30322 USA. He is also with the Biomedical Imaging Technology Center (BITC), 1639 Pierce Drive, Suite 2001, Atlanta, GA 30322 USA (e-mail: ymk@ieee.org).

A. El-Sharkawy is with the Electrical Engineering Department, The Johns Hopkins University, Baltimore, MD 21218 USA.

A. M. Youssef is with the Biomedical Engineering Department, Cairo University, Giza 12613, Egypt.

Digital Object Identifier 10.1109/TBME.2004.836501

Several techniques were proposed to perform motion artifact suppression, including automatic alignment techniques based on correlation and sum of absolute difference (cf. [1]–[5]). The motion encountered in this problem was classified into axial motion (motion in the direction of the beam) and lateral motion (in the direction perpendicular to the beam). The first was shown to be limited and possible to augment with the phase aberration correction problem [6]. That is, the solution to the phase aberration problem corresponds to the solution for both phase aberration and motion. On the other hand, special correlation processing was used to estimate the motion in the second direction by correlating neighboring lines. In spite of the encouraging results obtained, the computational complexity of such methods requires massive computing resources for real time implementation [3]. Therefore, it hinders such techniques from being applied to low-cost ultrasound systems.

In magnetic resonance imaging (MRI), the process for acquiring one image can last for a minute or more. As a result, motion artifacts are commonly encountered during long acquisition sequences as a result of motion of the imaged subject during the data collection period. In order to reduce this artifact, a technique called navigator echo was developed whereby a one-dimensional (1-D) projection of the image is collected with each acquisition [7]. These navigator echoes are registered together to estimate the translational motion in between acquisitions. Such estimates are subsequently utilized during the reconstruction process to compensate for this motion and yield images with much less motion artifacts.

Here, a similar technique to navigator echo motion estimation can be devised. In particular, the acquired raw ultrasound lines within a sub-aperture or one of the acquisitions can be used to obtain the equivalent of the navigator echo projection information indirectly. This is done using radial projection to sum all points on each line to obtain a 1-D signal as a function of line number representing the angle. The observation of this projection signal (or navigator echo) enables the estimation of motion in the lateral (angular) direction of the image. In this work, we present the theory and experimental verification of this approach when applied to synthetic aperture, interleaved, or averaged acquisition modes. This new technique is compared to the more computationally expensive approach based on optimizing a local information theoretic objective function during the reconstruction as a function of the motion parameter. Also, its performance is analyzed under different practical imaging conditions.

## II. THEORY

Consider the case of ultrasound imaging using a convex array transducer. Let the scanned image to be denoted as  $f(r, \theta)$  where  $\theta$  is the azimuth angle (or equivalently the line number) and  $r$  is the depth. Let the effective in-plane ultrasound transmit/receive field for a single acquisition line be defined as  $h(r, \theta)$ . Here, we assume no motion in the elevation direction of the transducer and, therefore, we will just consider the image formation in terms of the in-plane coordinates. Hence, the received ultrasound line  $s_1(r, \theta)$  takes the form

$$s_1(r, \theta) = \int f(r, \theta - \phi) \cdot h(r, \phi) d\phi. \quad (1)$$

Then, the sampled projection signal, or navigator echo, takes the form

$$P_1(\theta) = \Pi(\theta) \cdot \int s_1(r, \theta) dr \quad (2)$$

where  $\Pi(\theta)$  is the sampling function. In interleaved acquisition, the same aperture elements are used with different delays in a second run through the ultrasound array. This amounts to a different field function, which we will call here  $h_2(\theta)$  resulting in  $s_2(r, \theta)$  and  $P_2(r, \theta)$

as above. Let this field function incorporate any changes in the sampling position such that the sampling function remains unaltered. In this case, the correlation function of the two projection functions takes the form

$$C(\theta) = P_1(\theta) * P_2(-\theta). \quad (3)$$

The Fourier transform of the projection  $n$  where  $n = 1$  or  $2$ , takes the form

$$\mathfrak{F}\{P_n(\theta)\} = \Pi(k_\theta) * [\mathfrak{F}\{f(r, \theta)\} \cdot \mathfrak{F}\{h_n(r, \theta)\}]_{k_r=0}. \quad (4)$$

Here, we utilized the convolution property of the Fourier transform in addition to the projection-slice theorem to evaluate the projection as the center line of the two-dimensional (2-D) frequency domain, denoted by the variables  $(k_r, k_\theta)$ , at  $k_r = 0$ . Hence, assuming a motion of  $\Delta\theta$  in the second acquisition and sufficient sampling, the Fourier transform of the correlation function takes the form

$$\mathfrak{F}\{P_1(\theta)\} \cdot \mathfrak{F}\{P_2(-\theta)\} = \Pi(k_\theta) * (\mathfrak{F}\{f(r, \theta)\} \cdot \mathfrak{F}\{f(r, -\theta)\} \cdot \mathfrak{F}\{h_1(r, \theta)\} \cdot \mathfrak{F}\{h_2(r, -\theta)\} \cdot e^{-2\pi k_\theta \cdot \Delta\theta})_{k_r=0}. \quad (5)$$

By looking at the expression inside the parentheses, we notice that the first two terms will amount to a real function since the expression will be evaluated at  $k_r = 0$  and that they will be complex conjugates with respect to  $k_\theta$ . Also, we notice that two field terms are expected to be real with possible known linear phase term to account for sampling position given that the field is generally symmetric around the center of the acquisition line. Hence, by measuring the phase term of this multiplication, it is possible to detect and compute any misalignment between the two acquisitions.

Now consider the case of undersampling. This causes aliasing in the Fourier transform of each projection. Assume the undersampling factor (defined as the ratio of sampling frequency to that of Nyquist) to be given by  $\alpha$  and the true bandwidth of the signal to be  $B$ . Then, as long as  $\alpha$  is greater than 0.5, there will remain a part at the center of the Fourier transform without aliasing of size  $B(2\alpha - 1)$ . Since this linear phase estimation can still in principle be performed using a few points, the proposed approach can accommodate such undersampling and still provide correct motion estimates. Also, with the low-pass filtering caused by the diffracting ultrasound point spread function, the aliasing degree will be rather limited under practical imaging conditions.

In the most general case when one or both field functions are not symmetric, then the multiplication of their Fourier transforms may contain a nonlinear phase term. In this case, it is still generally possible to detect the motion by detecting the linear phase component of the nonlinear phase using least squares fitting. Another approach is to use a reference signal, which is more accurate but less practical. Moreover, if the two functions are not symmetric but reflected versions of each other with respect to  $\theta$  (i.e.,  $h_1(r, \theta) = h_2(r, -\theta)$ ), then their multiplication will result in a real-valued function of  $k_\theta$  from the time-reversal property of the Fourier transform. This means that the same method used in the symmetric case can still be used. Hence, the motion estimation using navigator echo should have a robust performance under this condition.

## III. METHODS

The angular motion estimate is computed by finding the shift corresponding to the maximum correlation of the two navigator echoes from consecutive interleaved acquisitions. This can be done by correlation in the spatial domain or by estimating the linear phase in the frequency domain from the middle few points around the zero frequency. The latter is preferred given its robustness against aliasing problems.

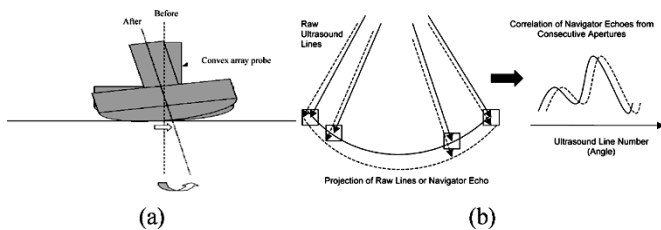


Fig. 1. Illustration of the navigator echo based technique. (a) Geometry of the system. (b) The projection of lines to generate the virtual navigator echoes.

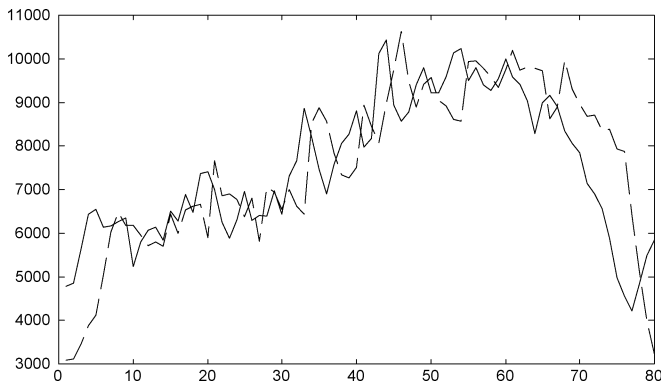


Fig. 2. Illustration of navigator echoes from two consecutive subapertures. The motion estimation is performed by matching the two navigator echoes.

When aliasing is not expected to be a problem, subsample interpolation techniques may be used in the spatial domain [11]. The final corrected image can subsequently be reconstructed after positioning the points from the second acquisition in their correct locations. Since the motion estimation step corresponds to simple 1-D correlation to detect a small shift relative the size of the array, its computational complexity is linear with the number of points in each acquisition. Therefore, it can be readily added to current reconstruction algorithms as a preprocessing step without affecting the overall order of computations. An illustration of this approach is shown in Fig. 1. A plot of actual navigator echo signals from two consecutive acquisitions is shown in Fig. 2. As can be seen, the two signals are generally similar in shape with a simple shift in between.

In order to verify the navigator echo approach, another class of optimal correction technique based on image quality focusing criteria was also implemented [8]. This class of methods was used in motion artifact suppression in MRI [8] and in phase aberration correction in ultrasound imaging [9] among other applications. The basic idea is to formulate an image quality objective function that relates directly to the motion parameters and optimize this measure (i.e., maximize or minimize depending on the formulation) to obtain the motion parameters that are most likely to have caused the present motion. Among the most commonly used objective function formulations for motion suppression is the one based on information theoretic criteria. A good example of this class is the entropy focusing criterion. The reconstructed image intensity varies according to the extent of the motion present. Therefore, we start with an initial estimate for the motion and perform the reconstruction and repeat the procedure with different estimates until the optimal shift value is obtained. This is done by taking advantage of the entropy measure preference of single strong peaks over the same peak energy distributed over a large area. Since the motion artifact itself can be modeled as blurring, this measure is very sensitive to motion artifacts and deteriorates rapidly with slight motion. Hence, minimization of the above criterion should provide an accurate estimate for the

motion parameter and consequently the sharpest reconstruction for an image. Nevertheless, the technique requires repeated reconstruction of the image regions to perform its iteration. This can be prohibitively slow in most cases. So, it is considered here as the “gold-standard” for correction that will be used to qualitatively evaluate the results from the navigator echo approach.

To quantitatively evaluate the performance of the new method against variations in the signal-to-noise ratio (SNR) as well as the effective bandwidth of the field function, simulations of the imaging experiment described above were performed to assess the motion estimation accuracy [10]. The resultant field was convolved with a numerical phantom that consists of a number of impulses to simulate wire targets and the result was projected to obtain the navigator echo. This process was performed for the odd lines first then the even lines simulating the process of interleaved acquisition for half element stepping. Relative shift between the even and odd field were simulated for 64 different values covering a range of values equivalent to  $\pm 8$  ultrasound lines. The shift between the navigator echoes corresponding to the even and odd fields was computed for each simulated shift under different conditions of SNR ranging between 10–30 dB. Here, the SNR was defined as the ratio between the impulse amplitude in the navigator echo to the standard deviation of noise in order to make this evaluation independent of the number of axial points in the simulation. Also, to investigate the robustness of the method against undersampling, different field functions with different aliasing characteristics were simulated to compare the three cases of no aliasing, 50% aliasing, and 90% aliasing. This investigation is important to evaluate the possibility of using this approach under practical sampling conditions.

#### IV. RESULTS AND DISCUSSION

An experiment was conducted whereby ultrasound imaging data were collected from a New Sonics Compact clinical ultrasound imaging scanner (International Electronics—Biomedical Division, Egypt) using a 96-element convex array transducer of 3.5-MHz center frequency, 0.9-mm element size, and 60% relative bandwidth. The image reconstruction in this system is based on PC-based computing platform utilizing Intel PIII 600-MHz processor and 128-MB RAM. The scanning method involved interlacing two frames of different aperture sizes of 15 and 16 elements to form a higher resolution reconstruction based on a half-element step. The field of view depth was 16 cm. The hardware of this low-end system did not allow the real-time aperture size change to enable normal sequential acquisition without sacrificing the frame rate. Interleaved acquisition was used to scan the even lines first then the odd changing the aperture size only between them rather than with every line. The line acquisition time was  $350 \mu\text{s}$  and the number of lines in each frame was 80. The two available apertures were swapped each frame to collect a whole frame with each aperture. A general purpose B-mode imaging phantom (AIUM standard compliant, CIRS, Inc., Norfolk, VA) was scanned using this system once while fixing the probe on the phantom and then while applying subtle in-plane probe motion. The ultrasound system was configured to store the raw lines in a buffer that was dumped into a data file after the acquisition is completed for off-line processing. This processing included motion estimation in addition to image reconstruction and display.

Fig. 3 illustrates a B-mode scan using a stationary probe. The image is free of artifacts. On the other hand, with a simple movement of the probe, artifacts such as the image in Fig. 4 appear. The data for this figure were corrected using the navigator echo approach and the entropy focusing based approach. Fig. 5 shows the corrected images using the navigator echo approach, while the results from the entropy focusing appear in Fig. 6. As can be seen in both images, the blurring

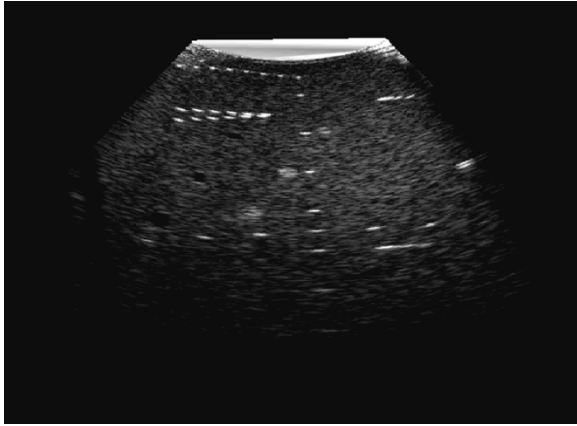


Fig. 3. Original phantom image without motion artifacts.

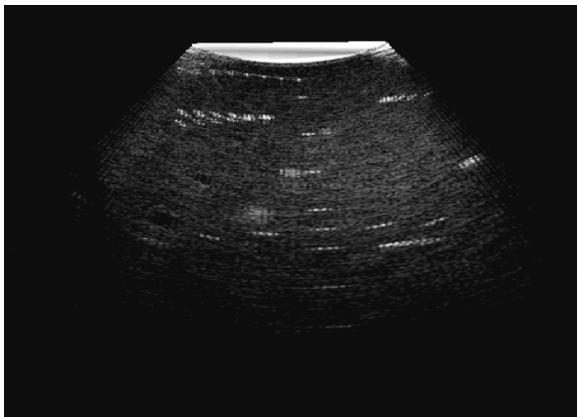


Fig. 4. Motion-corrupted phantom image.

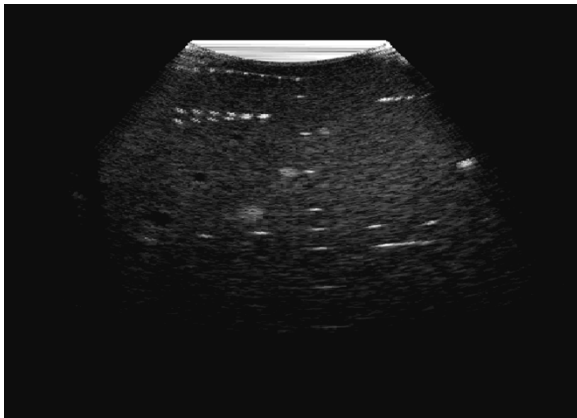


Fig. 5. Corrected image with the navigator echo approach.

inside the image has been reduced significantly. The quality of correction was examined visually by a number of independent observers (10 for this particular image). The observers were given a binary decision to make whether the processing resulted in an improvement or not. This qualitative approach was used given that quantitative measures are prone to bias from the ultrasound speckle on difference images reconstructed based on different estimated motion values. All observers noted the improvement. The differences in correction of different areas (e.g., the side pins) between the two corrected images were also reported but with general conclusions that they both have a generally similar image quality. With the simplicity and speed of computation of the navigator echo approach, this result illustrates the potential of this

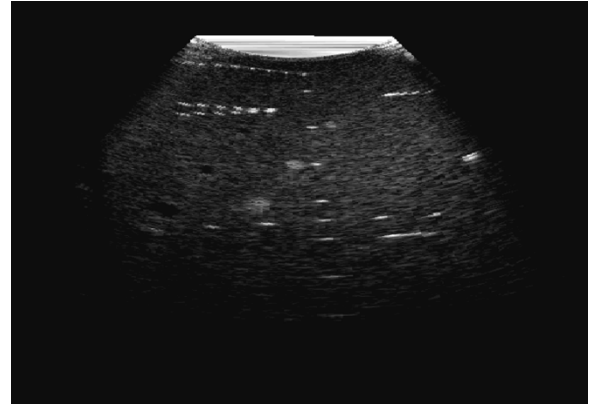


Fig. 6. Corrected image using entropy focusing.

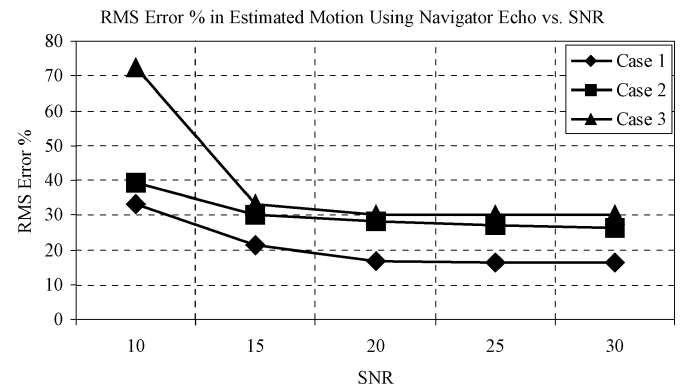


Fig. 7. RMS motion estimation error percentage versus SNR for three simulated cases: case 1 of no aliasing, case 2 of 50% aliasing, and case 3 of 90% aliasing.

approach for use in real-time image reconstruction as well as confirms the validity of the model used.

The results of the simulation experiment are shown in Fig. 7 where the root-mean-square (rms) error percentage is plotted. The rms error percentage was defined as the percentage of rms of the difference between the estimated and correct displacements relative to the correct displacement based on all 64 shift values simulated. The performance of the new method under navigator echo SNR values at or below 10 dB was observed to be not good. Given that the navigator echo signal is computed by adding points along the radial direction of the image, the SNR of the navigator echo is expected to be much better than that of the actual ultrasound image. Hence, it is expected that the navigator echo SNR will always be above 10 dB. Also, we observe that the different degrees of aliasing affect the estimation accuracy. This is mainly due to the fact that practical frequency domain functions are not compact in general. So, even though the middle part of the frequency domain is not aliased, bringing the aliases closer to the fundamental spectrum tends to add more errors to this part as a result of adding the tails of such functions. This explains the deterioration of performance when such aliasing increases.

In this experiment, the motion was mainly observed in the angular direction with both techniques. Moreover, the absence of axial (radial) motion was a common feature in all of our experiments. It is indeed possible to perceive a situation where this is possible when more pressure is applied toward the tissues. However, this would result in a nonrigid type of motion that is not possible to address using the new method. In other words, the motion estimation using navigator echo can be performed only in the angular direction.

The problem formulation in ultrasound imaging has several unique features as compared to MRI. First, the navigator echo in ultrasound

imaging is virtual, unlike with MRI where real echo that may be different from the image data is collected. Second, the motion in ultrasound imaging almost exclusively happens in the direction of the probe elements (i.e., simple lateral shift in linear array imaging and angular shift in convex array imaging). Even though the classical navigator echo approach is limited to simple shift in one dimension, this does not pose any limitations on its use in ultrasound imaging where the actual motion follows this 1-D motion model closely.

Since the motion is estimated using a linear fit of the phase of a few points around the center of the Fourier domain, the Fourier transform is computed only for these points rather than the entire spectrum. Consider the case of acquiring  $N$  lines with  $M$  samples each. Hence, the number of points in the navigator echo is  $N$  points. Since each point in the discrete Fourier transform requires  $O(N)$  computations and that the phase slope estimation from a few points requires a much less computational effort, the motion estimation is expected to still be  $O(N)$ . Even with the total computations including  $M \cdot N$  additions to compute the navigator echo data, the implementation of this part did not affect the real-time frame rate of our system (approximately 1 ms/frame extra). This is in sharp contrast to the use of 2-D correlation, which incurs as many computations as the reconstruction process itself per lag (at least an order of magnitude more than our method), or the entropy focusing method, which extends at least an order of magnitude beyond that. Therefore, in principle, the inclusion of the navigator echo approach into the reconstruction process is possible. However, this mandates that other changes in the reconstruction process be implemented to accommodate the requirements of motion correction. For example, most ultrasound imaging systems utilize a reconstruction table to speed up the calculation of the image. Such tables are built under the assumption of fixed data point locations. Once motion is present, the change in the locations of some of the data points renders the available reconstruction table unusable. Since the number of subapertures is usually small, we can envision having a number of reconstruction tables representing different relative motions between subapertures. This issue remains open for future work.

It should be noted that the new method addresses well the situation where the motion in the image is the result of probe motion. This is mainly because this case is an ideal example for rigid-body motion. We have not addressed the problem of tissue motion given that this usually involves spatially-variant motion models that cannot be estimated using the current methodology. Future work may include development of spatially-localized variants of the navigator echo approach where correlation is performed with only a local subset of the points on the navigator echo instead of globally using the whole signal.

## V. CONCLUSION

A new technique for motion artifact suppression in synthetic aperture ultrasound imaging was developed. This technique is based on navigator echo and was shown to be suitable for real-time reconstruction while providing comparable results to the optimal entropy focusing method. Therefore, it can be used to make the current synthetic aperture more robust in addition to extending the use of this technology in lower-cost ultrasound systems. Moreover, it can be used with other more general strategies that utilize multiple acquisitions to form a single image such as averaging of frames and interleaved acquisition.

## REFERENCES

- [1] G. E. Trahey and L. F. Nock, "Synthetic receive aperture imaging with phase correction for motion and for tissue inhomogeneities—part I: basic principles," *IEEE Trans. Ultrason., Ferroelect., Freq. Contr.*, vol. 39, pp. 489–495, July 1992.
- [2] L. F. Nock and G. E. Trahey, "Synthetic aperture imaging in medical ultrasound with correction for motion artifacts," in *Proc. 1990 IEEE Ultrason. Symp.*, 1990, pp. 1597–1601.
- [3] B. Tavli and M. Karaman, "Correlation processing for correction of phase distortions in subaperture imaging," *IEEE Trans. Ultrason., Ferroelect., Freq. Contr.*, vol. 46, pp. 1477–1488, Nov. 1999.
- [4] M.-H. Bae and M.-K. Jeong, "Bidirectional pixel based focusing in conventional B-mode ultrasound imaging," *Electron. Lett.*, vol. 34, no. 22, pp. 2105–2107, 1998.
- [5] J.-S. Jeong, J.-S. Hwang, M.-H. Bae, and T.-K. Song, "Effects and limitations of motion compensation in synthetic aperture techniques," in *Proc. 2000 IEEE Ultrasonics Symp.*, vol. 2, Oct. 2000, pp. 1759–1762.
- [6] S. W. Flax and M. O'Donnell, "Phase-aberration correction using signals from point reflectors and diffuse scatterers: basic principles," *IEEE Trans. Ultrason., Ferroelect., Freq. Contr.*, vol. 35, no. 6, pp. 758–767, 1988.
- [7] Y. Wang, R. C. Grimm, J. P. Felmlee, S. J. Riederer, and R. L. Ehman, "Algorithms for extracting motion information from navigator echos," *Magn. Reson. Med.*, vol. 36, pp. 117–123, 1996.
- [8] D. Atkinson, D. L. G. Hill, P. N. R. Stoyale, P. E. Summers, and S. F. Keevil, "Automatic correction of motion artifacts in magnetic resonance images using an entropy focus criterion," *IEEE Trans. Med. Imag.*, vol. 16, pp. 903–910, Dec. 1997.
- [9] L. Nock and G. E. Trahey, "Phase aberration correction in medical ultrasound using speckle brightness as a quality factor," *J. Acoust. Soc. Amer.*, vol. 85, no. 5, pp. 1819–1833, 1989.
- [10] J. A. Jensen, "Field: a program for simulating ultrasound systems," *Med. Biol. Eng. Comp.*, Suppl. 1, Part 1: Proc. 10th Nordic-Baltic Conf. Biomed. Eng., vol. 4, pp. 351–353, 1996.
- [11] I. Cespedes, Y. Huang, J. Ophir, and S. Spratt, "Methods for estimation of subsample time delays of digitized echo signals," *Ultrason. Imag.*, vol. 17, pp. 142–171, 1995.